JOURNAL OF VIROLOGY, Dec. 1994, p. 8239–8253
0022-538X/94/$04.00+0

Vol. 68, No. 12

Characterization of Marek's Disease Virus Insertion and Deletion Mutants That Lack US1 (ICP22 Homolog), US10, and/or US2 and Neighboring Short-Component Open Reading Frames†

MARK S. PARCELLS,[1] AMY S. ANDERSON,[2] JOHN L. CANTELLO,[2] AND ROBIN W. MORGAN[2]*

School of Life and Health Sciences, College of Arts and Sciences,[1] and Department of Animal Science and Agricultural Biochemistry, College of Agricultural Sciences,[2] University of Delaware, Newark, Delaware 19717-1303

Received 24 June 1994/Accepted 21 September 1994

We report the characterization of Marek's disease virus (MDV) strains having mutations in various genes that map to the unique short (US) region of the viral genome. A deletion mutant (GAΔ4.8*lac*) lacks 4.8 kbp of US region DNA, the deleted segment having been replaced by the *lacZ* gene of *Escherichia coli*. This deletion results in the loss of the MDV-encoded US1, US10, and US2 homologs of herpes simplex virus type 1, as well as three putative MDV-specific genes, Sorf1, Sorf2, and Sorf3. Two mutants containing *lacZ* insertions in the US1 and US10 genes have been constructed, and we have previously reported a US2*lac* insertion mutant (J. L. Cantello, A. S. Anderson, A. Francesconi, and R. W. Morgan, J. Virol. 65:1584–1588, 1991). The isolation of these mutants indicates that the relevant genes are not required for growth of MDV in chicken embryo fibroblasts. The mutants had early growth kinetics indistinguishable from those of their parent viruses; however, 5 to 7 days after being plated, the US1 insertion mutant (US1*lac*) and the GAΔ4.8*lac* deletion mutant showed a 5- to 10-fold decrease in virus growth. This decrease in virus accumulation correlated with a 30 to 50% decrease in plaquing efficiency when these viruses were plated onto established versus fresh chicken embryo fibroblast monolayers compared with a 10 to 15% decrease seen for the parent viruses and for the US10*lac* or US2*lac* insertion mutants. Finally, GAΔ4.8*lac* could be reisolated from chickens, indicating that the deleted genes are not required for the infection of chickens following intra-abdominal inoculation of an attenuated serotype 1 MDV.

Marek's disease virus (MDV) is an avian herpesvirus that rapidly induces T-cell lymphomas following infection of susceptible chickens (8). Although MDV has been classed as a gammaherpesvirus on the basis of its biological properties, its genome organization and sequence as presently known indicate that it should be grouped among the alphaherpesvirus (5–7). Many MDV genes have been identified and mapped on the basis of homology of the gene products to known alphaherpesvirus proteins. Genes that map to the unique short (US) region of the genome include the US1 (5, 6), US2 (5, 6, 9, 33, 35), US3 (5, 6, 33, 35), US6 (glycoprotein D [gD]) (5, 6, 33, 35), US7 (glycoprotein I [gI]) (5, 6, 33), and US8 (glycoprotein E [gE]) (5, 6) genes and several open reading frames unique to MDV called short-component open reading frames (Sorfs) 1, 2, 3, and 4 (5, 6). Although these genes have been identified, mapped, and sequenced, a protein gene product has been identified in only a few cases, and in no case is gene function understood.

The genetics of alphaherpesvirus US regions is best characterized for herpes simplex virus type 1 (HSV-1). Of 13 HSV-1 genes that map to the US region, 12 have been reported to be nonessential for virus propagation in cell culture (17, 23). The term nonessential usually refers to a particular cell culture system and does not necessarily mean that a gene product is nonessential in all cell types, in experimental animals, or in the natural host. Even though gene products are nonessential in some cell culture systems, they may have critical functions under other circumstances since many are reasonably highly conserved among alphaherpesviruses. MDV offers an attractive system with which to examine the functions of nonessential gene products in the natural host.

The MDV US1 gene encodes a homolog of the HSV-1 US1 product (also known as ICP22, α22, or IE68) (5). ICP22 homologs are encoded by bovine herpesvirus 1 (38), equine herpesvirus 1 (EHV-1) (18, 41), equine herpesvirus 4 (EHV-4) (10), HSV-2 (45), herpesvirus of turkeys (HVT) (46), pseudorabies virus (PrV) (47), and varicella-zoster virus (VZV) (11, 12). Except for HSV-1, HSV-2, HVT, and MDV, all identified US1 homolog genes map within the inverted repeats flanking the US region and, therefore, many herpesviruses are diploid for the gene (10–12, 18, 47). The MDV US1 gene product has a predicted molecular mass of approximately 20 kDa. On polyacrylamide gels, the MDV US1 protein migrates as species of 24 and 27 kDa because of posttranslational modifications (5, 6). HSV-1 ICP22 is a 68-kDa nuclear phosphoprotein (14, 15), and phosphorylation appears critical for HSV-1 ICP22 activity (32). In addition, the HSV-1 protein is modified by adenylylation and/or guanylylation in isolated nuclei of infected cells (3).

The kinetic class of US1 homologs varies among herpesviruses. The HSV (14, 45) and bovine herpesvirus 1 (38) US1 genes are classified as immediate-early. Similarly, the VZV ICP22 homolog (IE63) is a putative immediate-early protein (20). In contrast, the US1 homologs of EHV-1 (18), PrV (47),

* Corresponding author. Mailing address: Department of Animal Science and Agricultural Biochemistry, University of Delaware, Newark, DE 19717-1303. Phone: (302) 831-2524. Fax: (302) 831-8177. Electronic mail address: robin.morgan@mvs.udel.edu.

† Miscellaneous paper 1532 of the Delaware Agricultural Experiment Station, Newark, Del.

and MDV (5, 6) are expressed later in infection. The EHV-1 US1 homolog (ORF4) is transcribed into two differentially expressed transcripts predicted to encode proteins 293 and 469 amino acids in length that share carboxy termini homologous to the carboxy terminus of HSV-1 ICP22 (18). One of the transcripts (1.4 kb) is predominant early in infection, and the other (1.7 kb) appears late in infection. The kinetic class of PrV US1 has not been characterized other than as not being an immediate-early RNA (47). Finally, the MDV US1 protein appears to be expressed late in infection and localized to the cytoplasm of infected duck embryo fibroblasts (5, 6).

The function of US1 is not understood, but studies on mutant viruses indicate that the degree of essentiality of US1 for HSV-1 varies among cell culture systems (see Discussion). In mice, HSV-1 US1 mutants show a decrease in lethality following intracerebral inoculation (39). Such mutants can establish latency in mice inoculated via the eye but do so less efficiently than parental HSV-1.

The MDV US2 homolog was originally sequenced by Cantello et al. and was predicted to encode a protein with a molecular mass of 32,400 Da (9). Homologs of the US2 gene of HSV-1 have been identified in HSV-2 (25), VZV (11, 12), PrV (43), and EHV-1 (41). The US2 protein of HSV-1 contains a hydrophobic N-terminal region and may be membrane associated (24). Mutant viruses lacking US2 have been isolated for HSV-1 (22, 44), PrV (13), and MDV (9), indicating that the genes are nonessential for growth in cell culture in these systems.

The US10 gene of HSV-1 encodes a 33-kDa protein (24). Homologs to the US10 protein are encoded by HSV-2 (4), VZV (12), EHV-1 (41), EHV-4 (10), and MDV (5, 6, 35). US10 homologs contain a potential zinc finger domain, which suggests a role in DNA binding (19). Mutants that lack US10 and can replicate in cell culture have been reported for HSV-1 (21, 42) and HSV-2 (4).

Sorf1 and Sorf2 are unique to MDV (5, 6), and at present, it is not known whether they are expressed. Sorf2 shows homology to an uncharacterized fowlpox open reading frame, ORF4 (5, 6). A homolog to Sorf3 has recently been identified in HVT (40, 46).

This report describes the construction of MDV insertion mutants containing *lacZ* insertions in either the US1 or the US10 gene and a mutant containing a *lacZ* insertion in a 4.8-kbp deletion within the US region. This deletion removes six genes, including MDV US1, US10, and US2 genes. The characterizations of these mutants as well as that of a previously reported US2*lac* insertion mutant (9) are presented.

MATERIALS AND METHODS

Cells and viruses. MDV was propagated in secondary chicken embryo fibroblasts (CEF) with growth medium consisting of M199 medium (Life Technologies, Inc. [LT], Grand Island, N.Y.), 100 IU of penicillin G per ml, and 100 μg of dihydrostreptomycin per ml (27). Mutants were constructed by use of passage level 75 (GAatt75) and 85 (GAatt85) of the GA strain of MDV.

Plasmid constructions. Plasmids pMD162 and pMD189 were used to make US1*lac* and US10*lac* insertion mutants, respectively, and were constructed as follows (Fig. 1). The 2.8-kbp *Eco*RI subfragment of *Bam*HI-A was ligated into the *Eco*RI site of pMD160, a modified pUC18 vector in which the *Sal*I site was deleted from the multiple cloning region and the *lacZ* α-peptide reading frame was maintained. The resulting plasmid, pMD161, contained a unique *Sal*I site located 231 nucleotides (approximately 40%) into the coding region of the MDV US1 gene (5) (Fig. 1C). Plasmid pMD161 was digested with *Sal*I and blunt ended by use of the Klenow fragment of *E. coli* DNA polymerase I (LT). A *lacZ* cassette (Fig. 1D), derived from pCH110 (Pharmacia, Inc., Piscataway, N.J.) and modified for insertion mutagenesis (40), was blunted and ligated into pMD161. The resulting plasmid (pMD162) was used to construct the US1*lac* insertion mutant. For the construction of the US10*lac* insertion mutant, plasmid pMD189 was generated by digestion of pMD161 with *Nae*I, which cleaves 90 bp (approximately 14%) into the US10 coding sequence (5), and the blunt-ended *lacZ* cassette was inserted into the *Nae*I site (Fig. 1C).

Plasmid pMD190 was constructed in order to generate the MDV deletion mutant (GAΔ4.8*lac*) as follows (Fig. 1C). A 12.2-kbp *Hin*dIII-*Bam*HI fragment of *Bam*HI-A was cloned into the *Hin*dIII-*Bam*HI sites of pUC18 to generate pMD163. Plasmid pMD163 was digested with *Pst*I, and the 10.4-kbp fragment containing vector sequences was purified by preparative agarose gel electrophoresis and self-ligated to generate pMD164 (not shown). pMD164 was digested with *Pst*I and blunt ended by use of the Klenow enzyme (LT), and the blunt-ended *lacZ* cassette was inserted into the former *Pst*I site to generate pMD190 (Fig. 1C). This deletion results in (i) the removal of 96 bp (corresponding to 32 amino acids or 36%) from the 5′ end of Sorf1 including all of the upstream region, (ii) the deletion of the entire coding sequences of Sorf2, US1, US10, and Sorf3, and (iii) the removal of 651 bp (217 amino acids or 80%) from the US2 coding region.

The *lacZ*-containing plasmids, pMD162, pMD189, and pMD190, were purified by the Qiagen maxi-preparation procedure (Qiagen Corp., Chatsworth, Calif.). Disruptions of the US1 and US10 open reading frames were confirmed by the dideoxy sequencing method with Sequenase I (United States Biochemical Corporation, Cleveland, Ohio) and primers homologous with the ends of the *lacZ* cassette.

US1*lac*, US10*lac*, and GAΔ4.8*lac* MDV strain constructions. The US1*lac*, US10*lac*, and GAΔ4.8*lac* mutants were constructed via cotransfection of plasmid and MDV-infected cell DNA as detailed previously for a US2*lac* mutant MDV (9).

Southern hybridizations. For Southern blot analysis, 10 μg of DNA from MDV-infected CEF was digested with *Stu*I in the cases of US1*lac* and US10*lac* and with *Eco*RI for GAΔ 4.8*lac* (Fig. 2 and 3). DNA fragments were separated on 0.6% agarose gels, transferred to nitrocellulose, and detected by hybridization according to standard procedures (36). The MDV-specific probes used for Southern analysis were subfragments of the *Bam*HI-A fragment of a GA strain genomic library constructed by Fukuchi et al. (16) (Fig. 2C and 3B). The *lacZ*-specific probe was a 2.1-kbp *Bgl*I fragment contained within the coding sequence of the *lacZ* cassette (Fig. 1D). Probe DNA fragments were gel purified and labelled with [α-^{32}P]dCTP by random primed DNA labelling (United States Biochemical).

Northern (RNA) hybridization. Total RNA was purified by the guanidinium isothiocyanate method for RNA purification followed by cesium chloride step gradient centrifugation (2). RNA preparations were treated with RNase-free RQ1 DNase (Promega Biotech, Madison, Wis.) and quantitated by A_{260}. Unless otherwise indicated, 10 μg of total RNA from each sample was used for Northern blot analysis. Molecular size markers used were RNA ladders (Promega). Blots were prepared and hybridized by standard procedures (2). The MDV-specific DNA and RNA probes used for analysis are shown in Fig. 4A. To produce strand-specific probes, the 0.8-kbp *Bgl*II-*Sal*I fragment of pMD163, the 0.5-kbp *Stu*I fragment of

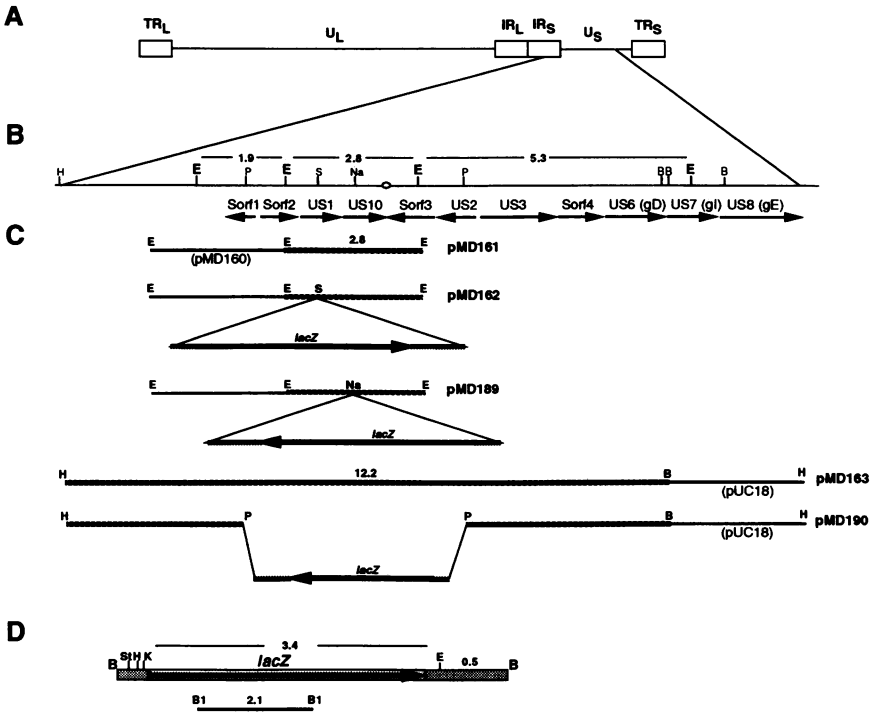

FIG. 1. Plasmid constructions used for the generation of recombinant MDV strains. (A) Diagram of the structure of the MDV genome. (B) Diagram of the US region of the MDV genome including a restriction map generated from *Bam*HI-A and -P_1 fragment clones (19), a map of the encoded open reading frames (5, 6), and the sizes (in kilobase pairs) of *Eco*RI fragments spanning the region of interest. (C) Linear maps of the plasmids generated for the construction of recombinant MDV strains. Hatched bars represent subfragments of the *Bam*HI-A clone of the MDV genome (19). Solid bars indicate plasmid sequences. Triangles containing cross-hatched bars and solid arrows indicate the sizes and orientations of *lacZ* cassette insertions. (D) Diagram of the *lacZ* cassette used for mutagenesis. The 2.1-kbp *Bgl*I fragment depicted below the cassette was used to probe for the *lacZ* gene and its expression. Shaded bars flanking the solid arrow denote simian virus 40 DNA sequence. Abbreviations: U_L, unique-long region; TR_L, terminal repeat flanking the U_L; IR_L, internal repeat flanking the U_L; U_S, unique-short region; IR_S, internal repeat flanking the U_S; TR_S, terminal repeat flanking the U_S; B, *Bam*HI; Bl, *Bgl*I; E, *Eco*RI; H, *Hin*dIII; K, *Kpn*I; Na, *Nae*I; P, *Pst*I; S, *Sal*I; St, *Stu*I.

pMD160, and the 1.1-kbp *Eco*RI-*Bgl*II fragment of pMD100 (9) were subcloned into pGEM vectors (Promega) to yield pMD165 (pGEM4Z), pMD166 (pGEM3Z), and pMD167 (pGEM3Z), respectively (Fig. 4A). Riboprobes were generated by use of either T7 or SP6 polymerase as noted in the legend of Fig. 4. Blots hybridized with riboprobes were washed with 2× SSC (1× SSC is 0.15 M sodium chloride and 0.015 M sodium citrate, pH 7) containing 1 μg of RNase A (Sigma Chemical Co., St. Louis, Mo.) per ml for 15 min at room temperature followed by two washes of 0.1× SSC containing 0.1% sodium dodecyl sulfate at 65°C to reduce nonspecific hybridization of the probe to rRNA.

Immunofluorescence staining. Tissue culture dishes (60 mm diameter) of mock- or MDV-infected CEF were incubated for 6 to 7 days until cytopathic effects were visible in MDV-infected cultures. Monolayers were fixed by the addition of 95% ethanol to the dishes, which were then stored at −20°C until staining. Prior to use, dishes were rehydrated and rinsed three times with wash solution consisting of phosphate-buffered saline (PBS) containing 3% heat-inactivated calf serum (LT). Antiserum against the MDV US1 protein was prepared and provided by P. Brunovskis and L. Velicer, Michigan State University, East Lansing, Michigan. Affinity-purified antiserum against β-galactosidase was provided by Calvin Keeler, University of Delaware, Newark, Delaware, or obtained commercially (5 Prime→3 Prime, Inc., Boulder, Colo.). Prior to use, both antisera were diluted 1:100 in diluent consisting of PBS containing 3% goat serum (Sigma). For staining, dishes were incubated with 2 ml of antibody solution for 2 h at 37°C and subsequently rinsed three times with PBS. Dishes were then incubated for 1 h at 37°C with 2 ml of fluorescein isothiocyanate-conjugated goat anti-rabbit immunoglobulin G antiserum (Sigma) diluted 1:100 in diluent. Finally, dishes were rinsed three times in wash solution and 2 ml of PBS was added to each dish. Fluorescent plaques were identified under UV illumination with an inverted-stage microscope (Nikon Inc., Tokyo, Japan) fitted with a DM 510 filter.

Growth curves. Twelve identical 60-mm tissue culture dishes of CEF were inoculated with GAatt75-, GAatt85-, US1*lac*-, US10*lac*-, US2*lac*-, or GAΔ4.8*lac*-infected CEF at approximately 100 PFU per dish. At 1, 2, 3, 5, and 7 days postinfection, monolayers were harvested from duplicate dishes and inoculated onto fresh CEF. Titer dishes were counted 6 days postinfection, and the mean number of plaques was determined. Growth curves for each virus were performed with CEF monolayers incubated at either 37 or 41°C, the latter being the body temperature of the chicken.

Plating on fresh versus established monolayers. Secondary CEF were prepared from primary CEF and plated onto 60-mm dishes. Two days later, additional secondary CEF were prepared from the initial stock of primary CEF. Monolayers infected with GAatt75, GAatt85, US1*lac*, US2*lac*, US10*lac*, or GAΔ4.8*lac* were harvested, and various doses of the viruses were plated in triplicate onto freshly prepared CEF, 2-day-old CEF, and 2-day-old CEF given fresh medium. Plaques were counted 6 days postplating, and the mean number of plaques

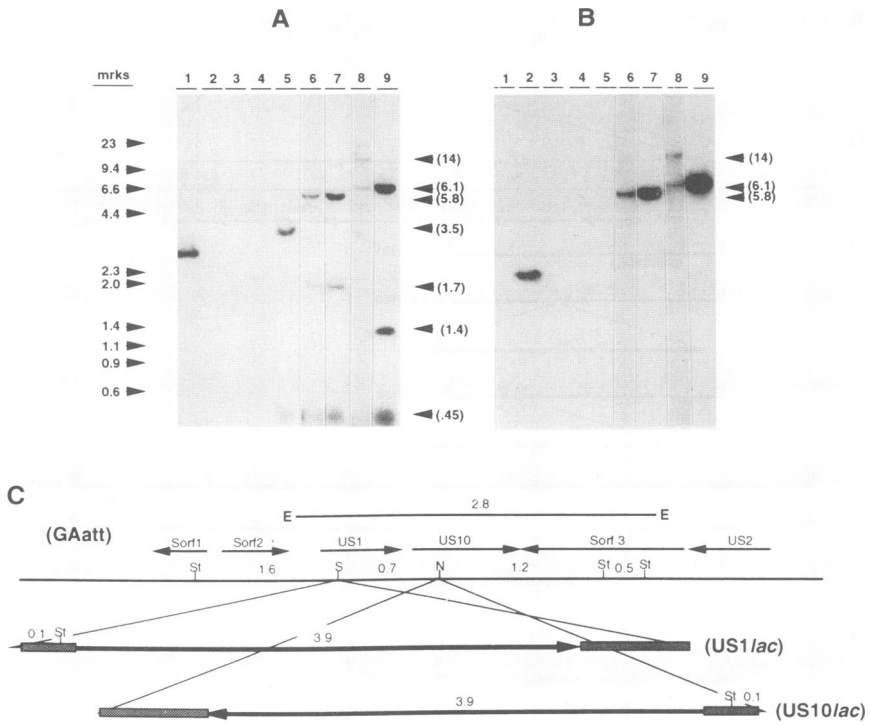

FIG. 2. Southern blot analysis of US1*lac* and US10*lac*. Panels A and B are Southern blots of *Stu*I-digested DNA. Lanes: 1, the 2.8-kbp *Eco*RI subfragment of the MDV US region (Fig. 1C, pMD161); 2, the 2.1-kbp *Bgl*I fragment of the *lacZ* cassette (Fig. 1D); 3, *Hin*dIII-digested λ DNA and *Hae*II-digested ΦX174 DNA markers; 4, uninfected CEF DNA; 5, GAatt85-infected CEF DNA; 6, US1*lac*-infected CEF DNA; 7, reisolated-US1*lac*-infected CEF DNA; 8, US10*lac*-infected CEF DNA; 9, reisolated-US10*lac*-infected CEF DNA. (A) Southern blot probed with the 2.8-kbp *Eco*RI fragment of pMD161 (shown in panel C). (B) Southern blot probed with the 2.1-kbp *Bgl*I *lacZ* fragment (see above). (C) Diagrams of the US regions of GAatt85, US1*lac*, and US10*lac* MDVs including the open reading frames, the *Stu*I sites, and the sites and orientations of *lacZ* insertion. Molecular sizes are given in kilobase pairs. Abbreviations: E, *Eco*RI; N, *Nae*I; S, *Sal*I; St, *Stu*I.

per dish was determined. The above procedure was performed several times, and the mean percentage decrease in plaque number on established CEF monolayers was determined for each virus strain.

Virus reisolations. One-day-old and seven-day-old specific-pathogen-free single-comb white leghorn chickens were obtained from SPAFAS (Norwich, Conn.), wingbanded, randomly assigned to experimental groups, and housed in modified Horsfall isolation units individually equipped with HEPA filters and maintained under negative pressure. At 1 or 7 days of age, chickens were inoculated intra-abdominally with various doses of GAatt75-, GAatt85-, US1*lac*-, US2*lac*-, US10*lac*-, or GAΔ4.8*lac*-infected or uninfected CEF, with five chickens for each inoculum. Spleen cells were isolated 5- to 7-days postinoculation as follows. Spleens were removed and pooled from three chickens per dose, rinsed in incomplete medium consisting of M199 (LT) supplemented with 100 IU of penicillin G per ml and 100 μg of dihydrostreptomycin per ml, and homogenized on ice with a Dounce homogenizer. Splenocytes were washed three times in incomplete medium and resuspended at a concentration of 2×10^7 cells per ml in complete medium (incomplete medium containing 3% heat-inactivated calf serum [LT]). For virus reisolations, 2×10^6 viable cells were plated onto fresh CEF and plaques were counted 6 days later. Cocultivation dishes for mutant viruses were stained for β-galactosidase activity as described previously (9).

RESULTS

Analysis of mutant genomes. Southern blots of *Stu*I-digested DNA from uninfected CEF or CEF infected with GAatt85, US1*lac*, reisolated US1*lac*, US10*lac*, and reisolated US10*lac* probed with the 2.8-kbp *Eco*RI subfragment of the *Bam*HI-A fragment of the MDV genome (Fig. 1) indicated that recombination of the *lacZ*-mutagenized MDV fragments in the GAatt85 genome occurred site specifically, in a manner consistent with a double reciprocal crossover (Fig. 2). The *lacZ* cassette used for mutagenesis contained an *Stu*I restriction site at its 5′ end and, therefore, introduced an additional *Stu*I site into the mutagenized region (Fig. 1). The presence of this additional *Stu*I site and the increase in apparent sizes of the MDV and *lacZ* homologous fragments indicated that the orientations of *lacZ* for US1*lac* and US10*lac* were as shown schematically in Fig. 2C. An additional band of approximately 14 kbp was detected in the DNA purified from US10*lac*-infected CEF. This band was absent in DNA purified from reisolated-US10*lac*-infected CEF. Digestion of DNA from US10*lac*-infected CEF with other restriction enzymes indicated that the 14-kbp fragment did not result from incomplete digestion with *Stu*I (data not shown).

Southern blot analysis of *Eco*RI-digested DNA purified from CEF infected with GAΔ4.8*lac* indicated that *lacZ* insertion occurred as depicted in Fig. 1 (Fig. 3). The *lacZ* cassette used for mutagenesis contained an *Eco*RI site (Fig. 1D), and insertion of the cassette into the deleted region resulted in the

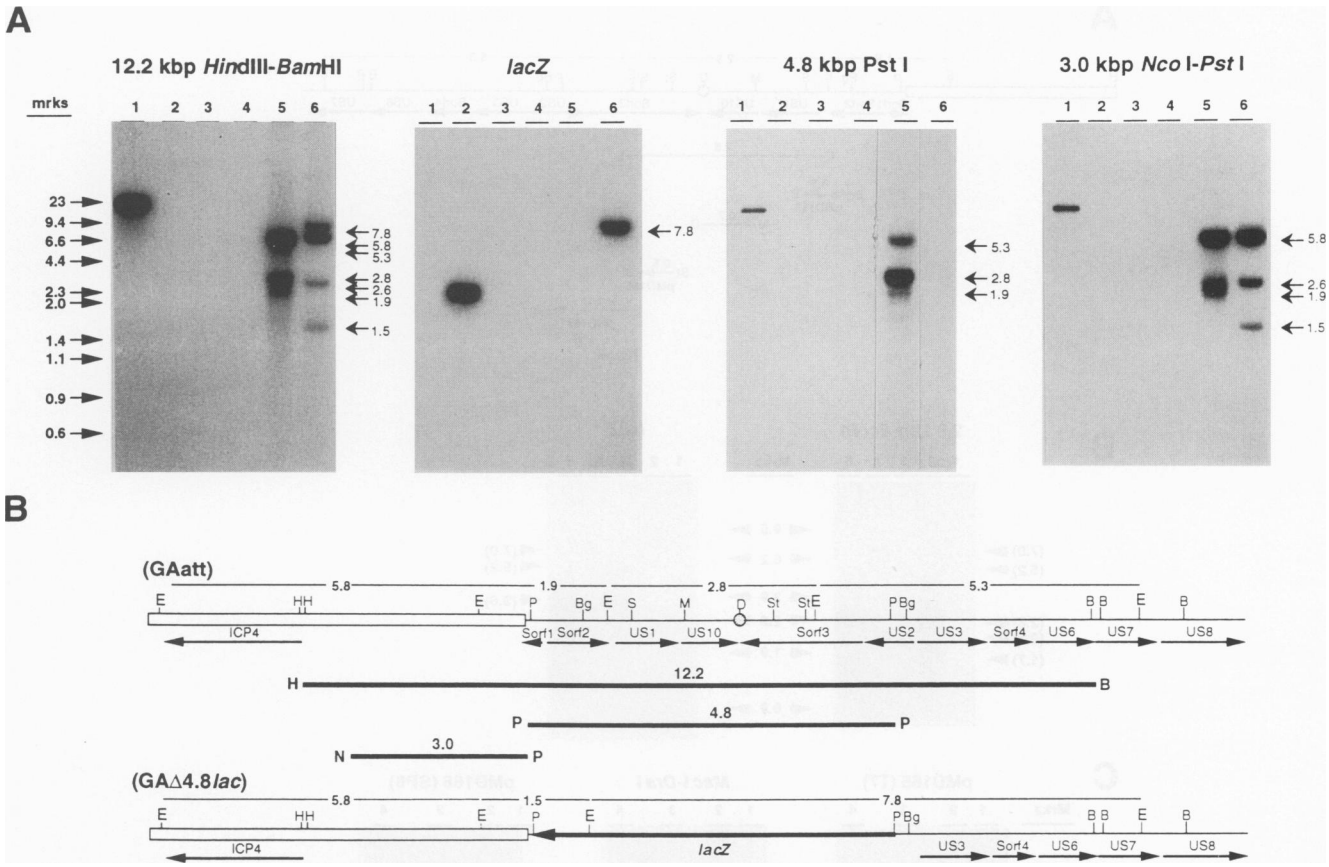

FIG. 3. Southern blot hybridization analysis of GAΔ4.8*lac*. (A) Southern blots of *Eco*RI-digested DNA. Lanes: 1, 12.2-kbp *Hin*dIII-*Bam*HI fragment of *Bam*HI-A; 2, 2.1-kbp *Bgl*I fragment of *lacZ* cassette; 3, *Hin*dIII-digested λ DNA and *Hae*III-digested ΦX174 DNA markers; 4, uninfected CEF DNA; 5, GAatt75-infected CEF DNA; 6, GAΔ4.8*lac*-infected CEF DNA. (B) Diagrams of the US regions of GAatt75 and GAΔ4.8*laclac* including restriction sites, open reading frames (labeled arrows), and the probes used in panel A (solid bars). The solid arrow indicates the site and orientation of *lacZ* cassette insertion in GAΔ4.8*lac*. The shaded circle denotes a prominent bidirectional transcriptional termination region. Sizes are given in kilobase pairs. Abbreviations: B, *Bam*HI; Bg, *Bgl*II; E, *Eco*RI; H, *Hin*dIII; P, *Pst*I, St, *Stu*I.

introduction of an *Eco*RI site. When the 12.2-kbp *Hin*dIII-*Bam*HI fragment spanning the deleted region was used as the probe for this analysis, bands of 5.8, 5.3, 2.8, 2.6, and 1.9 kbp were detected in GAatt75-infected CEF DNA (Fig. 3A). Bands of 7.8, 5.8, 2.6, and 1.5 kbp were detected in GAΔ4.8*lac*-infected CEF DNA (Fig. 3A). Deletion of the 4.8-kbp *Pst*I fragment and insertion of the 4.0-kbp *lacZ* cassette in GAΔ4.8*lac* should have resulted in the loss of the 2.8-kbp band, an increase in size of the 5.3-kbp band to 7.8 kbp, and truncation of the 1.9-kbp band to a species approximately 1.5 kbp in size. An unexpected band of 2.6 kbp was present in DNA from both the parent virus and the GAΔ4.8*lac* mutant. The *lacZ* probe detected the expected 7.8-kbp *Eco*RI fragment in GAΔ4.8*lac*-infected CEF DNA.

To examine the origin of the unexplained 2.6-kbp band, the blot probed with the *lacZ* fragment was stripped and reprobed with the 4.8-kbp *Pst*I fragment that constituted the deleted region (Fig. 3A). This analysis indicated that the 4.8-kbp *Pst*I fragment was indeed deleted from the GAΔ4.8*lac* genome and that no parental virus was present in the GAΔ4.8*lac* stock. We surmised that since the 12.2-kbp *Hin*dIII-*Bam*HI probe covered a portion of the internal repeat flanking the US (IR_S), the additional 2.6-kbp band could stem from hybridization of the probe to the *Eco*RI fragment spanning the junction between the US and the terminal repeat flanking the US (TR_S). The blot previously probed with the 12.2-kbp *Hin*dIII-*Bam*HI fragment was stripped and reprobed with a 3.0-kbp *Nco*I-*Pst*I fragment upstream of the site of *lacZ* insertion in GAΔ4.8*lac* and overlapping the internal repeat flanking the US (IR_S) (5). This probe detected the expected bands of 5.8 and 1.9 kbp in GAatt-infected CEF DNA and bands of 5.8 and 1.5 kbp in GAΔ4.8*lac*-infected CEF DNA (Fig. 3A). In addition, the probe detected the 2.6-kbp band in both GAatt- and GAΔ4.8*lac*-infected CEF DNAs. The results were consistent with the idea that the 2.6-kbp *Eco*RI fragment is the US-TR_S junction fragment.

Changes in MDV transcription due to mutagenesis. Changes in gene expression associated with the insertion of the *lacZ* cassette were examined by Northern blot hybridization (Fig. 4 and 5). A summary of the transcription analysis is presented in Fig. 6. The most prominent difference in transcription patterns between US1*lac*, GAΔ4.8*lac*, and their parent viruses was the loss of two abundant transcripts of 1.7 and 2.6 kb (Fig. 4B and 5B). Both these transcripts initiate upstream of the US1 open reading frame and are transcribed through the US1 and US10 open reading frames (Fig. 4C and 5B). The 2.6-kb transcript initiates just upstream of the *Pst*I site within the Sorf1 open reading frame (data not shown) and reads through Sorf1 and Sorf2, US1, and US10 open reading frames (Fig. 4C and 5B). The 1.7-kb transcript initiates to the

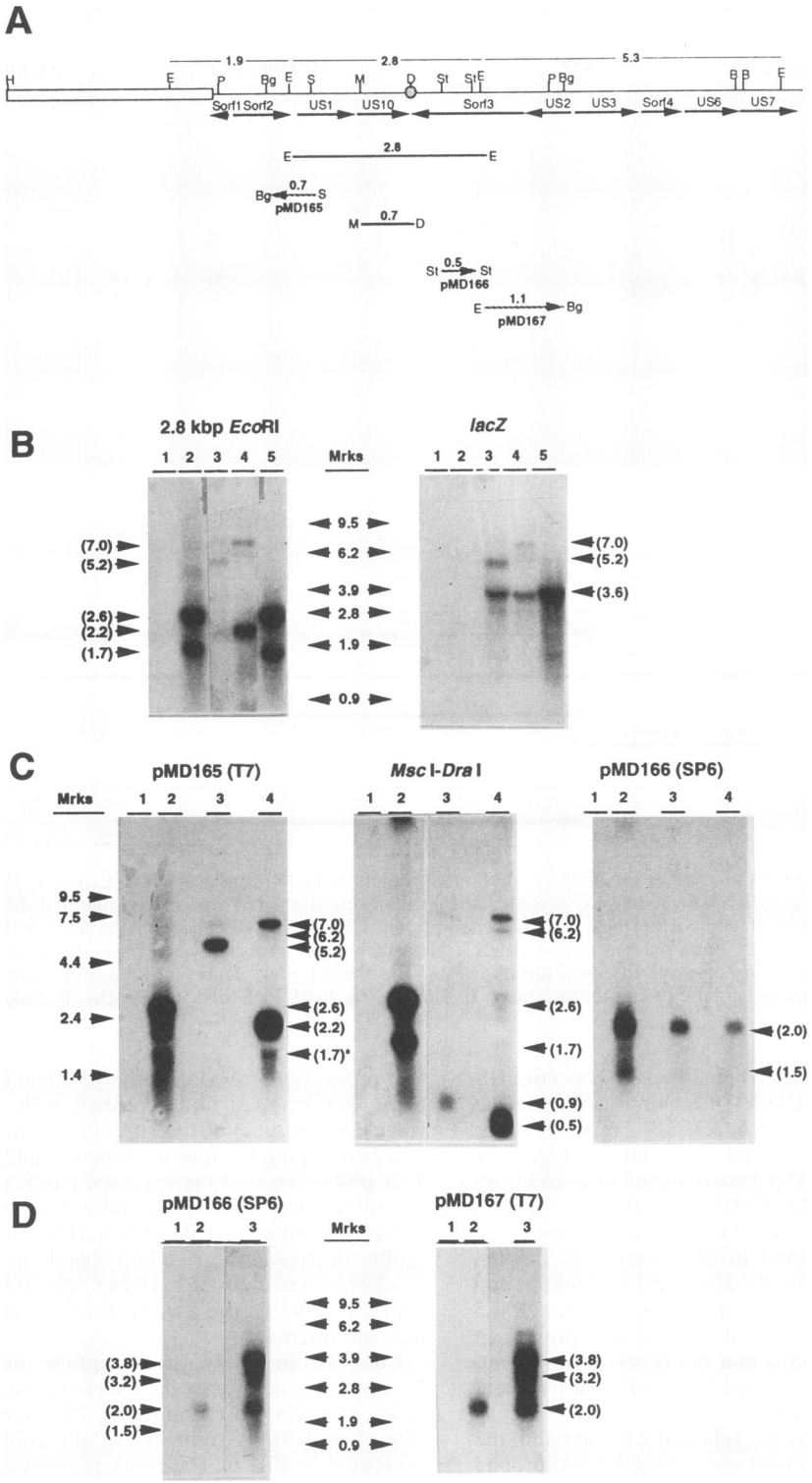

FIG. 4. Northern blot hybridization analysis of US1*lac*, US10*lac*, US2*lac*, and GAatt85 RNA. Transcription analysis was performed by Northern blot hybridization of total RNA. (A) Diagram of the US region of the MDV genome including a restriction map, the open reading frames, and the probes used for Northern blot analysis. Solid bars indicate double-stranded DNA probes. Hatched arrows indicate the locations and polarities of single-stranded riboprobes. The shaded circle denotes a prominent bidirectional transcriptional termination region. (B) Northern blots probed with the 2.8-kbp *Eco*RI fragment depicted in panel A or with the 2.1-kbp *Bgl*I fragment depicted in Fig. 1D. Lanes: 1, uninfected CEF RNA; 2, GAatt85-infected CEF RNA; 3, US1*lac*-infected CEF RNA; 4, US10*lac*-infected CEF RNA; 5, US2*lac*-infected CEF RNA. (C) Northern blots probed with a riboprobe derived from pMD165 with T7 polymerase, a 0.7-kbp *Msc*I-*Dra*I double-stranded DNA probe, or a riboprobe derived from pMD166 with SP6 polymerase. Lanes: 1, uninfected CEF RNA; 2, GAatt85-infected CEF RNA; 3, US1*lac*-infected CEF RNA; 4, US10*lac*-infected CEF RNA. The asterisk indicates the apparent 1.7-kb band present in GAatt-infected CEF but not in US1*lac*- or

right of the *Eco*RI site immediately upstream of the US1 open reading frame (Fig. 5B and reference 5). Although insertion of the *lacZ* cassette within the US1 open reading frame resulted in the loss of both transcripts, insertion within the US10 open reading frame resulted in the loss of the 1.7-kb transcript and truncation of the 2.6-kb transcript to a species approximately 2.2 kb in size (Fig. 4B and C). In Fig. 4C, the pMD165-derived riboprobe apparently detected a transcript species of approximately 1.7 kb. This band arose as an artifact of the RNase A wash protocol which preferentially digests riboprobes that hybridize nonspecifically to rRNA. Prior to the RNase wash, the US10*lac* RNA lane (Fig. 4C, pMD165, lane 4) contained a smear of RNA species which were presumably degradation products of the 2.2-kb transcript. After the RNase wash, the nonspecifically bound riboprobe digested from the rRNA bands left a visible gap in this smear of RNA species, creating what appeared to be a new transcript species just below the 18S rRNA. Since this transcript species was not detectable with a larger double-stranded probe which spans this region (Fig. 4B), with a double-stranded probe downstream of this region (Fig. 4C, *Msc*I-*Dra*I probe), or on subsequent blots probed with pMD165 (data not shown), it is unlikely that a transcript species of this size is expressed from this region of the US10*lac* genome.

The *lacZ* probe detected a major transcript of 3.6 kb, the expected size of the *lacZ* transcript, in RNA from CEF infected with US1*lac*, US10*lac*, US2*lac*, or GAΔ4.8*lac* (Fig. 4B and 5B). Expression of *lacZ* was constitutive in CEF infected with the mutant viruses, since the promoter driving *lacZ* expression on the insertion mutagenesis cassette was the simian virus 40 early promoter.

Several additional transcripts were also detected on the Northern blots (Fig. 4 and 5). First, a double-stranded *Msc*I-*Dra*I probe spanning the US10 open reading frame detected a low-abundance transcript of 0.9 kb in RNA from CEF infected with GAatt85 or the US1*lac* mutant that was truncated to a species of approximately 0.5 kb in RNA from US10*lac*-infected CEF (Fig. 4C). This low-abundance 0.9-kb transcript was not detected with larger probes or with probes upstream or downstream of US10 (Fig. 4B and C).

Second, minor-abundance transcripts of 5.2, 6.2, and 7.0 kb were detected in RNA purified from CEF infected with US1*lac* and/or US10*lac* but not with the parent virus (Fig. 4B and C). These large transcripts also hybridized with the *lacZ* probe (Fig. 4B). When US1*lac* RNA was probed with a riboprobe derived from pMD165, the 5.2- and 7.0-kb transcripts were detected, indicating that they result from promoter read-into and read-through of the inserted *lacZ* gene, respectively (Fig. 4B and C, schematically shown in Fig. 6B). The 5.2-kb transcript potentially encodes the amino-terminal 77 amino acids, or roughly 40% of the US1 protein. Likewise, the 7.0-kb transcript, which reads through the *lacZ* cassette and is detectable by the *Msc*I-*Dra*I double-stranded probe downstream of the site of *lac* insertion, potentially encodes the entire, albeit disrupted, US1 open reading frame. Whether portions of the US1 protein are translated, stable, or functional is unknown, but US1 protein expression is not detectable by the anti-US1-TrpE fusion protein antiserum used for immunofluorescence (Fig. 7).

Similarly, minor-abundance read-through transcripts of 6.2 and 7.0 kb were detected in RNA purified from US10*lac*-infected CEF. These transcripts were detectable both up- and downstream of the site of *lacZ* insertion, indicating that both transcripts read through the *lacZ* cassette (Fig. 4C). These transcripts potentially encode the amino-terminal 30 amino acids or roughly 14% of the US10 open reading frame which lies upstream of *lacZ* insertion. Because of a lack of antisera capable of detecting the MDV US10 protein by immunofluorescence, the expression of portions of this polypeptide cannot be excluded.

Third, a riboprobe derived from pMD166 and downstream of the US10 gene detected a transcript of 2.0 kb having the same polarity and possibly encoding US2 and/or Sorf3 products (Fig. 4C and D). This species was of minor abundance, and its detection by larger probes was masked by the abundance of the 2.6- and 1.7-kb transcripts mentioned above. The fact that this transcript was present in both GAatt85- and US10*lac*-infected CEF RNA indicated that disruption of the US10 open reading frame did not affect its expression. In addition, a 1.5-kb minor species which mapped to this region was inconsistently detected (Fig. 4C and D).

With regard to changes in US2 gene expression, Northern blot hybridization analysis with riboprobes generated from pMD166 and pMD167 (Fig. 4D), which are complementary to transcripts encoding the Sorf3 and US2 gene products, indicated that a transcript of 2.0 kb was present in RNA from GAatt85- and US2*lac*-infected CEF (Fig. 4D). In addition, species of approximately 3.8 and 3.2 kb were present in US2*lac*-infected CEF RNA. These transcripts apparently initiate within and are opposite in polarity to *lacZ*. Multiple transcripts having comparable sizes were detected with the double-stranded *lacZ* probe (Fig. 4B). Double-stranded probes derived from DNA sequences downstream of the US2*lac* site of *lacZ* insertion failed to detect the loss or truncation of any transcripts (data not shown).

Transcripts initiating within and antisense to *lac* were also detected downstream of the *lacZ* cassette insertion in GAΔ4.8*lac* (Fig. 5). These transcripts of >8 kb were detectable in long exposures of GAΔ4.8*lac*-infected CEF RNA hybridized with the *lacZ* probe (data not shown). These transcripts apparently read into a predominant 6.2-kb transcript that initiates just downstream or within the 5′ end of the US2 gene (Fig. 5B). This 6.2-kb species has been recently described (28) and reads through US3, Sorf4, US6, US7, and US8 genes to a transcriptional termination region near the US-TR_S junction (5).

Changes in MDV US1 protein expression due to mutagenesis. Immunofluorescence staining of GAatt85-, US1*lac*-, US10*lac*-, and GAΔ4.8*lac*-infected CEF indicated that the GAΔ4.8*lac* deletion mutant and the US1*lac* insertion mutant did not produce a US1 protein that reacted with the antiserum used, whereas the GAatt85 parent and US10*lac* insertion mutant did (Fig. 7). The loss of US1 protein expression indicated that no parental virus was present in the US1*lac* and GAΔ4.8*lac* stocks and correlated with the disruption or deletion of transcripts capable of encoding US1. The anti-US1 antiserum used for indirect immunofluorescence was generated against a fusion protein consisting of 123 amino acids, or approximately 69%, of the US1 protein fused to the TrpE

US10*lac*-infected CEF as discussed in the text. (D) Northern blots probed either with a riboprobe generated from pMD166 or a riboprobe derived from pMD167 (see above). Lanes: 1, uninfected CEF RNA; 2, GAatt85-infected CEF RNA; 3, US2*lac*-infected CEF RNA. Molecular sizes are given in kilobase pairs (DNA probes) or kilobases (RNA species and riboprobes); sizes of markers are shown in columns labelled mrks; observed transcript sizes are given in parentheses. Abbreviations used: B, *Bam*HI; Bg, *Bgl*II; D, *Dra*I; E, *Eco*RI; H, *Hin*dIII; M, *Msc*I; P, *Pst*I; S, *Sal*I; St, *Stu*I.

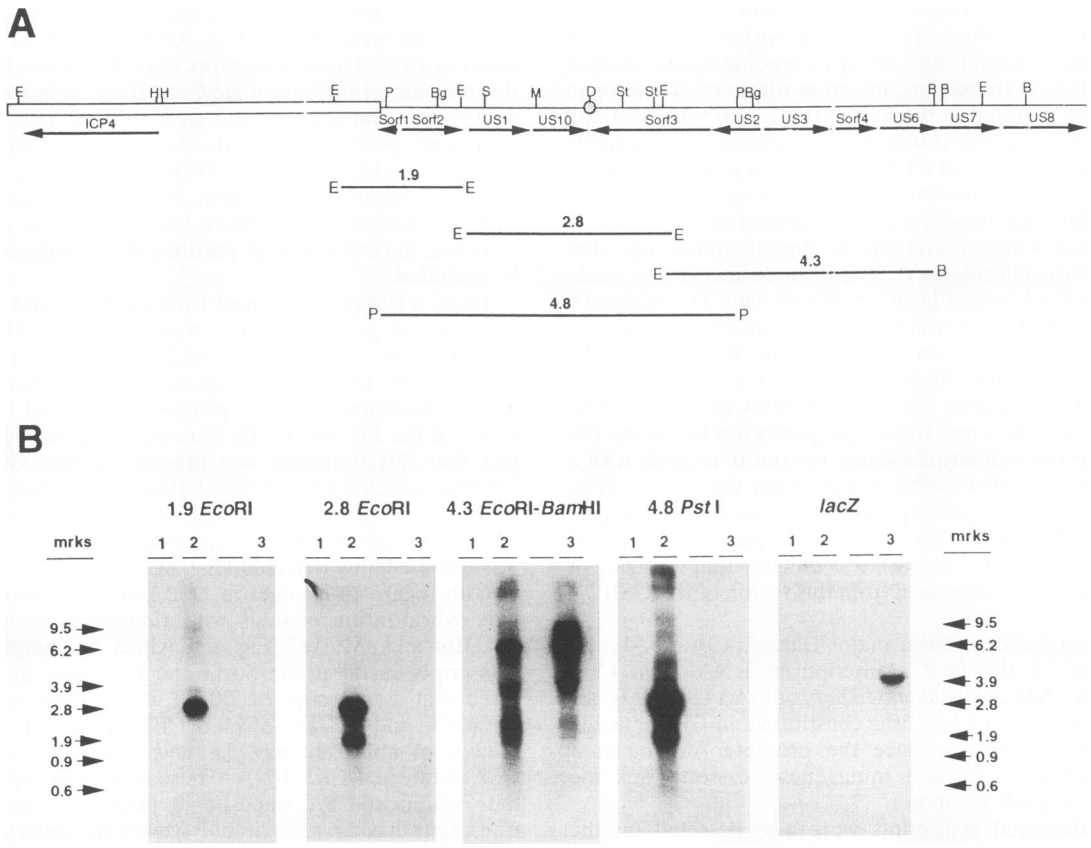

FIG. 5. Northern blot hybridization analysis of GAΔ4.8*lac* RNA. For Northern blot analysis, total RNA was used. (A) Diagram of the US region of MDV GA strain including a restriction map, a map of open reading frames, and the sizes and locations of probes used for the Northern blots. The shaded circle denotes a bidirectional transcriptional termination region. (B) Northern blots of MDV-infected CEF RNA. Lanes: 1, uninfected CEF RNA; 2, GAatt75-infected CEF RNA; 3, GAΔ4.8*lac*-infected CEF RNA. The probes are, as shown in panel A, the 1.9-kbp *Eco*RI subfragment of *Bam*HI-A, the 2.8-kbp *Eco*RI subfragment of *Bam*HI-A, the 4.3-kbp *Eco*RI-*Bam*HI subfragment of *Bam*HI-A, and the 4.8-kbp *Pst*I subfragment of *Bam*HI-A (constituting the region deleted from GAΔ4.8*lac*). The *lacZ*-specific probe is the 2.1-kbp *Bgl*I fragment of the *lacZ* cassette (Fig. 1D). Molecular sizes are given in kilobase pairs (DNA probes) or kilobases (RNA transcripts); mrks, markers. Abbreviations, B, *Bam*HI; Bg, *Bgl*II; D, *Dra*I; E, *Eco*RI; H, *Hin*dIII; P, *Pst*I; S, *Sal*I; St, *Stu*I.

protein of *Escherichia coli* (5, 6). An overlap of only 19 amino acids exists between the portion of US1 possibly expressed by US1*lac* and the portion of the US1 expressed as a TrpE fusion protein. Consequently, it is possible that US1*lac* expressed an amino-terminal fragment of the US1 protein that was not detectable by the anti-fusion protein antiserum. In the case of the GAΔ4.8*lac* deletion mutant, however, production of a truncated version of the US1 protein would be impossible. In addition, since the US10*lac* mutant produces immunologically detectable US1 and a truncated version of the 2.6-kb transcript, it is likely that the 2.6-kb transcript encodes US1. Immunofluorescence analysis with anti-β-galactosidase antibodies indicated the US1*lac*-, US10*lac*-, and GAΔ4.8*lac*-infected CEF expressed readily detectable levels of β-galactosidase whereas GAatt85-infected CEF did not (Fig. 7).

Loss of US1 affects the late but not the early growth kinetics of the US1*lac* and GAΔ4.8*lac* mutants in CEF. Growth curves of US1*lac*, US10*lac*, US2*lac*, and GAΔ4.8*lac* mutants showed that the loss of these genes either by singular disruption (US1, US10, and US2) or by deletion (Sorf1, Sorf2, US1, US10, Sorf3, and US2) caused no drastic growth impairment of MDV in CEF for the first 3 to 4 days postinfection (Fig. 8). For the US10*lac* and US2*lac* mutants, growth curves continued to be similar to those of their respective parent viruses for the duration of the experiment. Note that for the US10*lac* mutant 41°C growth curve, the input dose of US10*lac* was less than that of the GAatt85 parent virus and the two growth curves were essentially superimposable. However, differences in the growth curves of viruses lacking a functional US1 gene (US1*lac* and GAΔ4.8*lac*) became evident 4 to 6 days postinfection (Fig. 8). By 5 days postinfection at 41°C, both the US1*lac* insertion mutant and the GAΔ4.8*lac* deletion mutant showed decreases in virus accumulation resulting in at least 5- to 10-fold reductions in virus yield by day 7. This decrease was particularly notable for GAΔ4.8*lac*. Consistent with this result were the observations that US1*lac* and GAΔ4.8*lac* plaques were generally smaller than those of their respective parents and that the numbers of PFU per plaque that could be obtained upon passage of these strains were approximately 100 for US1*lac*, 50 for GAΔ4.8*lac*, and 200 for the parent viruses.

To determine whether the decreases in plaque size and virus yield observed for US1*lac* and GAΔ4.8*lac* were related to the growth status of the CEF monolayer, the plaquing efficiencies of the insertion mutants, the deletion mutant, and their respective parent viruses on freshly plated and established CEF monolayers were determined. Plating on 2-day-old CEF

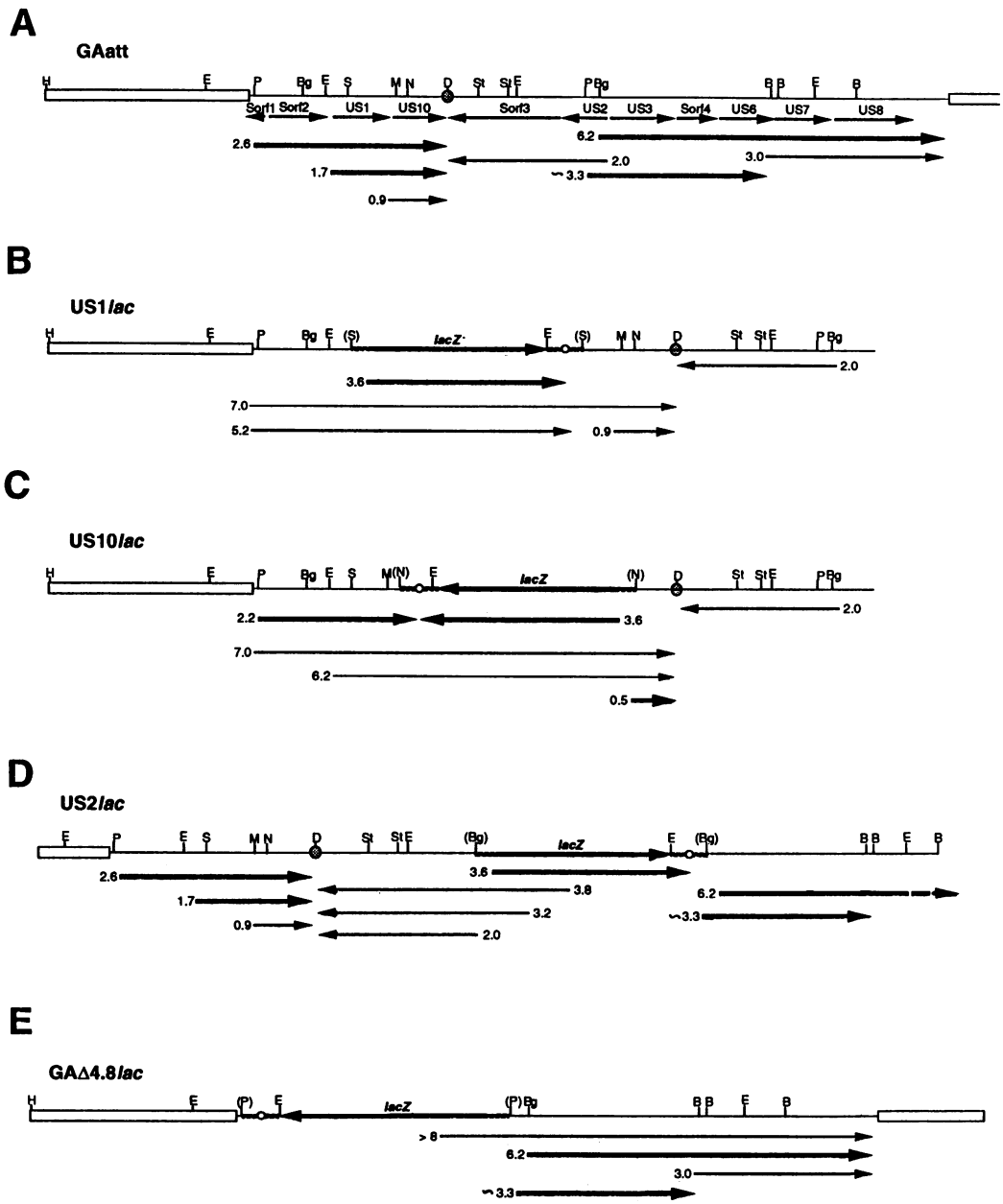

FIG. 6. Transcript maps of the US regions of GAatt, US1*lac*, US10*lac*, US2*lac*, and GAΔ4.8*lac*. Restriction and transcript maps are shown. The relative abundance of a transcript is shown by the width of the arrow presenting it. Since transcript mapping data were determined from RNA purified from MDV-infected CEF in the absence of metabolic inhibitors, the kinetic classes of RNAs cannot be inferred and some RNA classes may be absent or under- or overrepresented. The orientations and relative abundances of transcripts mapping to the left of the US2 gene were determined with double-stranded and strand-specific probes (Fig. 4 and 5). The orientations and abundances of transcripts mapping to the right of the US2 gene were determined previously (32). Transcriptional start and stop sites have been inferred from Northern blot hybridization analysis and the published DNA sequence of the region (5, 35). Circles denote prominent bidirectional transcriptional termination sites. Open boxes denote repeats flanking the US region. The *lacZ* cassette in the mutant strains is shown as a hatched bar containing a black arrow indicating the orientation of *lacZ* transcription. (A) Partial transcript map of the US region of the GA strain of MDV. (B) Transcript map of the US region of US1*lac* flanking the site of *lacZ* insertion. (C) Transcript map of the US region of US10*lac* flanking the site of *lacZ* insertion. (D) Transcript map of the US region of US2*lac*. Note that transcripts to the right of *lacZ* insertion are not drawn to scale. (E) Transcript map of the US region GAΔ4.8*lac*. Abbreviations: B, *Bam*HI; Bg, *Bgl*II; D, *Dra*I; E, *Eco*RI; M, *Msc*I; N, *Nae*I; P, *Pst*I; S, *Sal*I. Restriction sites in parentheses indicate that insertion of the *lacZ* cassette resulted in the disruption of the site.

monolayers resulted in a consistent 30 to 50% decrease in the number of US1*lac* and GAΔ4.8*lac* plaques obtained relative to the number of plaques obtained on fresh CEF cultures (Fig. 9). For the parent viruses and the US2*lac* and US10*lac* mutants, only a 10 to 15% decrease in plaque yield was noted (Fig. 9). The differences in plaquing efficiency between US1*lac*, GAΔ4.8*lac*, and their parent viruses could be ameliorated by the addition of fresh medium to the cultures prior to virus

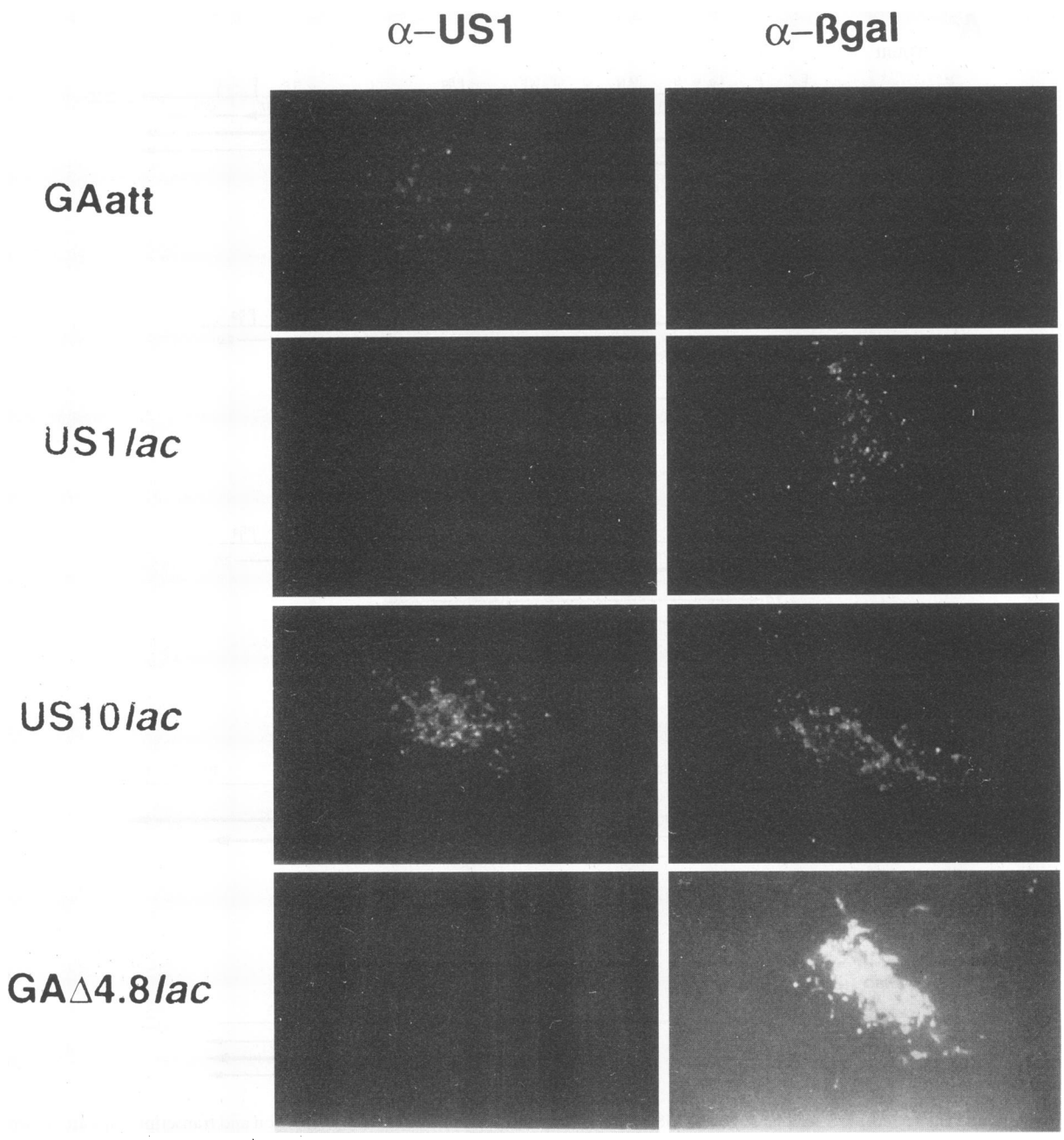

FIG. 7. Immunofluorescence analysis of GAatt85, US1*lac*, and GAΔ4.8*lac*. Ethanol fixed, MDV-infected monolayers were probed with either rabbit anti-US1-protein polyclonal antiserum (α-US1) or rabbit anti-β-galactosidase (α-βgal) followed by goat anti-rabbit-immunoglobulin-fluorescein isothiocyanate conjugate. Plaques shown are from GAatt85-infected CEF (GAatt), US1*lac*-infected CEF (US1*lac*), US10*lac*-infected CEF (US10*lac*), and GAΔ4.8*lac*-infected CEF (GAΔ4.8*lac*).

inoculation (data not shown). Furthermore, lymphoblastoid cell lines have been established from tumors induced by RB1BΔ4.8*lac*, an MDV mutant having a deletion identical to that of GAΔ4.8*lac* crossed into the genome of the highly oncogenic RB1B strain. When MDV was reactivated from these cell lines, a 30-fold growth impairment was seen on quiescent compared with freshly plated CEF (29).

Reisolation of MDV insertion and deletion mutants from infected chickens. For the input doses examined, the insertion and deletion mutants could be reisolated from spleen cells of infected chickens 5 to 7 days after intra-abdominal inoculation of virus-infected CEF (Table 1). In experiment 1, the reisolation frequency of US1*lac* was low and reisolation of US10*lac* was not detectable. In experiment 2, US10*lac* was reisolated at a frequency comparable with that of its parent virus and US1*lac* reisolation was apparent upon blind passage of the cultures. Since several experiments indicated that the GAΔ4.8*lac* mutant was efficiently reisolated and this strain carries a deletion spanning both the US1 and US10 genes, it was apparent that these genes are not essential for infection of chickens and

TABLE 1. Reisolation of mutant and parent viruses from splenocytes of chickens

Expt and strain	Dose (PFU)[a]	PFU/ (2×10^6 cells)[b]	Avg PFU/ (2×10^6 cells)[c]
1			
Mock infected		0, 0, 0	0 ± 0
GAatt75	11,000	8, 3, 4	5 ± 3
GAatt85	8,000	16, 13, 9	13 ± 4
US1*lac*	6,000	0, 1, 1	1 ± 1
US2*lac*	7,000	37, 47, 63	49 ± 13
US10*lac*	7,000	0, 0, 0	0 ± 0
GAΔ4.8*lac*	8,000	47, 33, 38	39 ± 7
2			
Mock infected		0, 0	0
GAatt75	30,000	4, 3	4
GAatt85	24,000	17, 13	15
US1*lac*	21,000	0, 0[d]	0[d]
US2.3*lac*	37,000	10, 12	11
US10*lac*	21,000	12, 7	10
3			
Uninfected		0, 0	0
Mock infected		0, 0	0
GAatt75	9,000	44, 45	45
US2*lac*	4,000	18, 31	25
GAΔ4.8*lac*	7,000	13, 7	10
4			
Uninfected		0, 0	0
Mock infected		0, 0	0
GAatt75	14,000	13, 8	11
US2*lac*	11,000	107, 137	122
GAΔ4.8*lac*	6,000	15, 18	17

[a] The indicated dose was inoculated intra-abdominally into specific-pathogen-free single-comb white leghorn chickens.
[b] Actual counts.
[c] Cocultivations were done in triplicate for experiment 1; values are means ± standard deviations. In other experiments, cocultivations were in duplicate.
[d] Virus was reisolated upon blind passage of the culture.

reisolation of viruses from splenic lymphocytes. Interestingly, the US2*lac* mutant was quite efficiently isolated in several experiments. However, in experiment 2, an independent US2 insertion mutant (US2.3*lac*) was tested, and this mutant was reisolated with efficiency comparable to that for its parent virus. Thus, disruption of the US2 gene does not appear to specifically enhance virus reisolation, and quantitative differences in reisolation frequencies may exist among independent isolates of mutants and should be interpreted with caution. All cocultivation dishes for mutant viruses stained positive for β-galactosidase activity, indicating that the Lac^+ phenotype was retained following passage of the strains through chickens.

DISCUSSION

We have constructed various MDV strains containing mutations that affect expression of the US1, US10, US2, Sorf1, Sorf2, and Sorf3 genes of an attenuated serotype 1 MDV. Southern blot analysis of DNAs from US1*lac*, US10*lac*, and GAΔ4.8*lac* viruses reisolated from splenocytes of infected chickens indicated that the reisolated mutant constructs were stable and free of parental virus (Fig. 2 and data not shown). The absence of detectable parental DNA restriction patterns in DNA from US1*lac* and GAΔ4.8*lac* mutants argues that the recombinant virus stocks are homogeneous at the sites of *lacZ* insertion. In the case of the original US10*lac* isolate, the detection of a 14-kbp band in *Stu*I-digested US10*lac* DNA with MDV- and *lacZ*-specific probes indicated the presence of an additional population of viruses containing an uncharacterized mutation as well as a *lacZ* cassette insertion. Failure to detect this population in US10*lac* that was reisolated from infected chickens indicates that the populations segregated during in vivo infection.

The construction of the insertion and deletion mutants demonstrates that the Sorf1, Sorf2, US1, US10, Sorf3, and US2 genes are nonessential for growth of attenuated MDV in CEF. This report and the reports that the US3 homolog (34) and US6 homolog (28) are nonessential indicate that 8 of the 11 putative genes encoded within the US region of MDV are nonessential for growth in cell culture.

The major changes in gene expression associated with the various mutants can be summarized as follows. (i) Insertion into the US1 gene of MDV resulted in the loss of two abundant transcripts 2.6 and 1.7 kb in size. These transcripts are likely to be the 2.6- and 1.7-kb species previously reported by Schat et al. (37). (ii) Insertion into the US10 gene of MDV resulted in the loss of the 1.7-kb transcript and truncations of the 2.6- and 0.9-kb transcripts to species that are 2.2 and 0.5 kb, respectively. (iii) Insertion into the US2 gene resulted in no detectable loss of transcripts and actually resulted in the presence of additional transcripts initiating within and antisense to the *lacZ* marker gene. The effects of these additional transcripts on MDV are unknown, but they clearly do not impair the growth of US2*lac* in cell culture or in vivo. (iv) Deletion of the 4.8-kbp *Pst*I fragment containing the 5′ end of the Sorf1 gene, the complete Sorf2, US1, US10, and Sorf3 genes, and 80% of the US2 gene resulted in the loss of the two predominant transcripts (2.6 and 1.7 kb) and the loss of several lower-abundance transcripts. Additionally, insertion of the *lacZ* cassette into this deletion resulted in the expression of large transcripts (>8 kb) initiating within and antisense to the *lacZ* gene. These transcripts extended through US3, Sorf4, US6, US7, and US8 genes of MDV and presumably terminates at or near the US-TR_S junction.

Other changes in transcription involve transcripts that originate upstream of the *lacZ* insertion site and read through the *lacZ* cassette. Although these read-through transcripts are of minor abundance, they do present the possibility that portions of the US1 and US10 proteins may be produced. These transcripts could possibly be translated to yield portions of the US1 (40%) or US10 (14%) proteins. Since the antiserum used to detect the US1 protein by immunofluorescence may not detect such a truncated protein (see above), it is possible that a portion of the US1 protein is expressed in US1*lac*-infected CEF. Likewise, it is possible that a portion of the US10 protein and a portion of the US2 protein are expressed in US10*lac*- and US2*lac*-infected CEF, respectively. However, it is not possible that the GAΔ4.8*lac* mutant produces truncated versions of US1 or US10 proteins, since their entire coding regions have been deleted.

Of the mutants constructed, the US1 mutants (US1*lac* and GAΔ4.8*lac*) were the most interesting phenotypically. Growth curves indicated that production of these mutant viruses was affected late, but not early, after plating. In addition, the use of 2-day-old CEF cultures resulted in a 30 to 50% decrease in plaque yields obtained with these mutants compared with a 10 to 15% decrease for the parent and the US2*lac* and US10*lac* mutant viruses. These results suggested that a factor present in freshly prepared CEF may be able to compensate for the loss of US1. In older CEF cultures, typical of the later stage of the growth curves, this factor may be less abundant or less active, making the effect of US1 loss appear more apparent in the

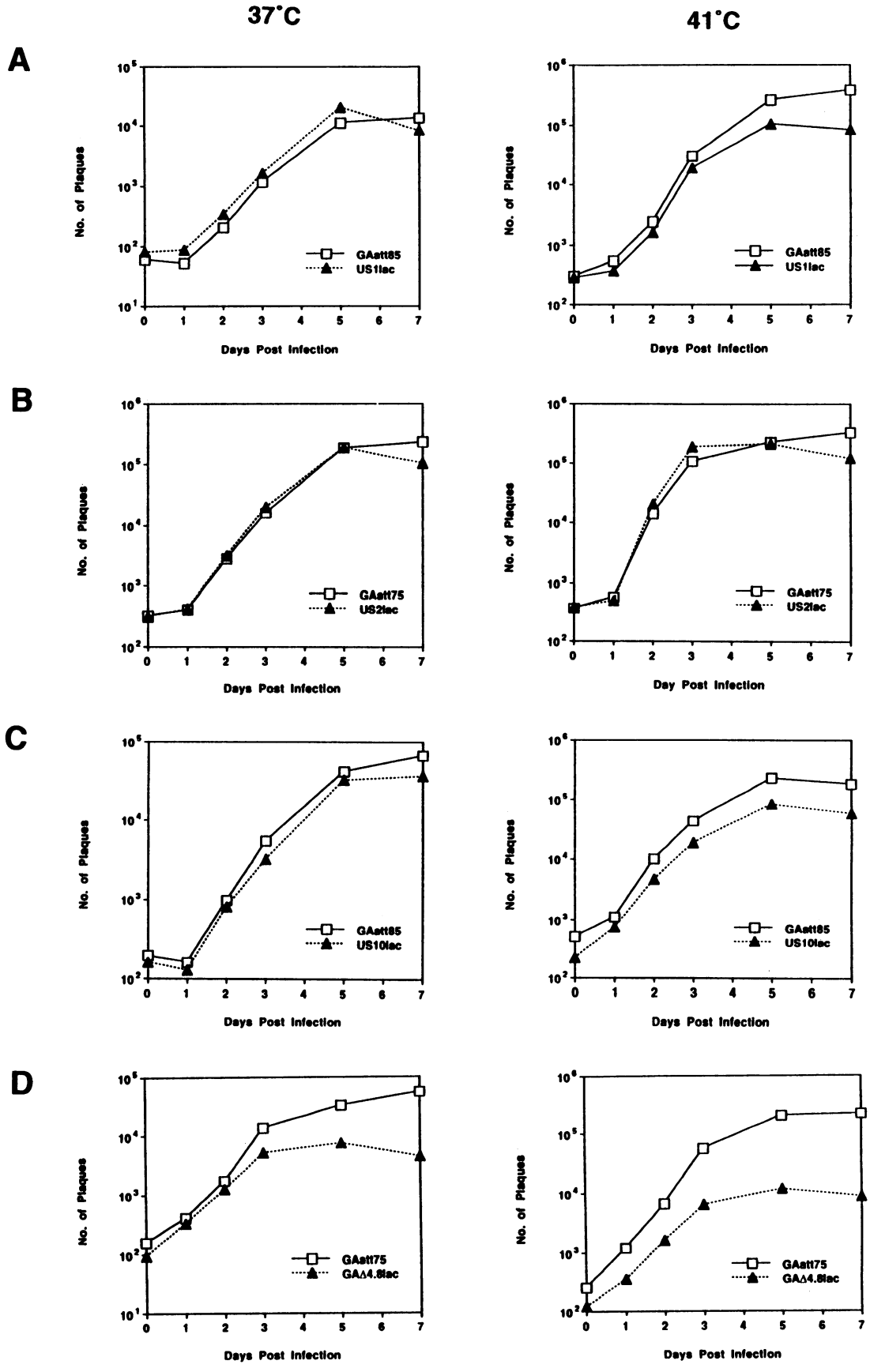
37°C
41°C
A
B
C
D
No. of Plaques
Days Post Infection
Day Post Infection
GAstt85
US1lac
GAstt75
US2lac
US10lac
GAΔ4.8lac

FIG. 8. Mutant MDV growth curves. Growth curves were performed at 37°C or at 41°C. Parent viruses are indicated by squares, and mutant viruses are indicated by solid triangles. Time points are means of at least two dilutions plated in triplicate per virus strain. Growth curves are GAatt85 versus US1*lac* (A), GAatt75 versus US2*lac* (B), GAatt85 versus US10*lac* (C), and GAatt75 versus GAΔ4.8*lac* (D).

growth kinetics, plaque size, and PFU-per-plaque ratio. That a cellular factor present in some cell types may compensate for the loss of US1 is consistent with studies on HSV-1 US1 (ICP22) (30, 31, 39). An HSV-1 mutant lacking the carboxy-terminal two-thirds of ICP22, R325βtk$^+$, grew in Vero cells but showed restricted growth in human embryonic lung cells and RAT-1 rodent cells (1, 31, 39). This mutant produced a truncated amino-terminal portion of ICP22 of approximately 33 kDa that was localized to the nucleus (1). Another mutant, containing a deletion of all but 18 nucleotides of the US1 coding region, had similar growth properties in these cells (30). Both mutants displayed prolonged expression of several early gene products and delayed accumulation of late gene products (30, 39), suggesting that ICP22 is involved somehow in the early-to-late shift in virus gene expression.

The nature of the putative cellular compensatory factor is unknown at this time. One report suggested that the cellular factor may be more efficient or be regulated differently from the HSV-1 US1 protein (39). This hypothesis was based on the fact that a gamma promoter was expressed earlier in permissive cells infected with HSV-1 lacking US1 than in cells infected with intact HSV-1, presumably because of the greater efficiency of the cellular compensatory factor in the absence of viral US1. The hypothesis may also be supported by the fact that HSV-1 lacking US1 actually initially grew better in permissive Vero cells when plated at high multiplicities of infection (39). In the case of MDV, the putative cellular factor appeared to be more efficient in actively growing CEF cultures than in 2-day-old cultures in which the monolayers were completely confluent. Interestingly, when growth curves were done for an HSV-1 US1 mutant, it was reported that although growth was restricted in actively growing human embryonic lung cells, growth restriction appeared to be dependent on the age of the cultures (39).

The observed phenotype for the US1 mutants was more pronounced for the GAΔ4.8*lac* deletion than for the US1*lac* insertion mutant. It is possible that the insertion mutant produced a truncated version of US1 derived from the portion of the gene upstream of the insertion site, and this truncated version of the protein may have some activity. If MDV and HSV-1 US1 proteins are functionally equivalent, this is unlikely since the initial HSV-1 US1 deletion mutant isolated produced a truncated version of US1 comprised of approximately one-third of the US1 protein (1) and this mutant displayed a host range and general phenotype like those of a more-recently isolated deletion mutant in which all but 18 nucleotides of the HSV-1 US1 gene was deleted (30). Alternatively, other genes missing in the GAΔ4.8*lac* mutant may have subtle phenotypes relative to viral growth that are not obvious in the individual mutants but become apparent when combined with loss of US1. That virulence is multigenically controlled has been reported for pseudorabies virus (26).

The successful reisolation of GAΔ4.8*lac* from splenocytes of chickens inoculated intra-abdominally with the virus argues that the deleted genes are not absolutely required for early infection of chickens by an attenuated MDV. However, this result does not rule out the possibility that the genes contribute to virulence in vivo in some cell types or under certain circumstances. A more thorough investigation of the in vivo phenotypes of these mutants involving other tissues such as neural tissue is in progress. In addition, we have recently isolated a deletion mutant in the background of the RB1B oncogenic strain of MDV (RB1BΔ4.8*lac*) (29), and this mutant should be revealing with regard to the influence of the relevant US genes on early cytolytic infection, oncogenicity, and horizontal spread of the virus.

ACKNOWLEDGMENTS

We thank Peter Brunovskis and Leland Velicer for sharing sequence data and antisera and for helpful conversations, Sandra Cloud for

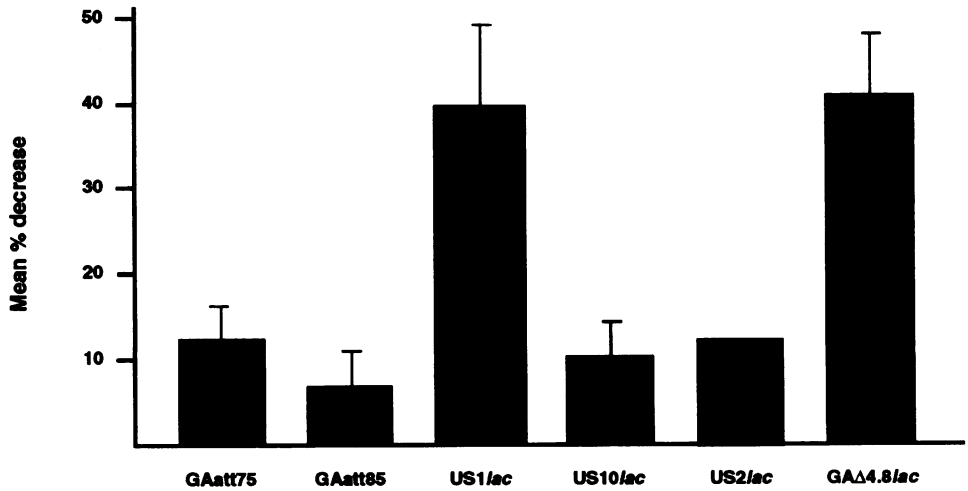

FIG. 9. Mean decrease in plaquing efficiency of MDV strains on established (2-day-old) CEF monolayers. The bars represent the mean percent decreases in the numbers of plaques counted when identical inocula were plated onto 2-day-old versus freshly plated CEF monolayers. With the exception of US2*lac*, five to seven trials were performed for each virus strain. Error bars represent standard deviations; no standard deviation bar is shown for US2*lac* since only two trials were performed.

assistance with the in vivo experiments, Calvin Keeler for antibodies to β-galactosidase, and Paul Sondermeijer for the *lacZ* cassette.

This work was supported by the Delaware Research Partnership; Intervet International, Boxmeer, The Netherlands; and American Cancer Society grant VM-44.

REFERENCES

1. **Ackermann, M., M. Sarmiento, and B. Roizman.** 1985. Application of antibody to synthetic peptides for characterization of the intact and truncated α22 protein specified by herpes simplex virus 1 and the R325 $\alpha22^-$ deletion mutant. J. Virol. **56:**207–215.
2. **Ausubel, F. M., R. Brent, R. E. Kingston, D. D. Moore, J. G. Seidman, J. A. Smith, and K. Struhl (ed.).** 1987. Current protocols in molecular biology. John Wiley & Sons, New York.
3. **Blaho, J. A., C. Mitchell, and B. Roizman.** 1993. Guanylylation and adenylylation of the α regulatory proteins of herpes simplex virus require a viral β or γ function. J. Virol. **67:**3891–3900.
4. **Brown, S. M., and J. Harland.** 1987. Three mutants of herpes simplex virus type 2: one lacking the genes US10, US11, and US12 and two in which R_S has been extended by 6 kb to 0.91 map units with loss of U_S sequences between 0.94 and the U_S/TR_S junction. J. Gen. Virol. **68:**1–18.
5. **Brunovskis, P.** 1992. Identification and characterization of Marek's disease virus unique short region genes and their products. Ph.D. thesis. Michigan State University, East Lansing.
6. **Brunovskis, P., and L. F. Velicer.** 1992. Genetic organization of the Marek's disease virus unique short region and identification of U_S-encoded polypeptides, p. 74–78. Proc. 19th World's Poultry Congress. Ponsen & Looijen, Wageningen, The Netherlands.
7. **Buckmaster, A. E., S. D. Scott, M. J. Sanderson, M. E. G. Boursnell, N. L. J. Ross, and M. M. Binns.** 1988. Gene sequence and mapping data from Marek's disease virus and herpesvirus of turkeys: implication for herpesvirus classification. J. Gen. Virol. **69:**2033–2042.
8. **Calnek, B. W., and R. L. Witter.** 1991. Marek's disease, p. 342–385. *In* B. W. Calnek (ed.), Diseases of poultry. Iowa State University Press, Ames.
9. **Cantello, J. L., A. S. Anderson, A. Francesconi, and R. W. Morgan.** 1991. Isolation of a Marek's disease virus (MDV) recombinant containing the *lacZ* gene of *Escherichia coli* stably inserted within the MDV US2 gene. J. Virol. **65:**1584–1588.
10. **Cullinane, A. A., F. J. Rixon, and A. J. Davison.** 1988. Characterization of the genome of equine herpesvirus 1 subtype 2. J. Gen. Virol. **69:**1575–1590.
11. **Davison, A. J.** 1983. DNA sequence of the U_S component of the varicella-zoster virus. EMBO J. **2:**2203–2209.
12. **Davison, A. J., and J. E. Scott.** 1986. The complete DNA sequence of varicella-zoster virus. J. Gen. Virol. **67:**1759–1816.
13. **de Wind, N., A. Zijderveld, K. Glazenburg, A. Gielkens, and A. Berns.** 1990. Linker insertion mutagenesis of herpesviruses: inactivation of single genes within the US region of pseudorabies virus. J. Virol. **64:**4691–4696.
14. **Fenwick, M., M. Walker, and L. Marshall.** 1980. Some characteristics of an early protein (ICP22) synthesized in cells infected with herpes simplex virus. J. Gen. Virol. **47:**333–341.
15. **Fenwick, M. L., M. J. Walker, and J. M. Petkevich.** 1978. On the association of virus proteins with the nuclei of cells infected with herpes simplex virus. J. Gen. Virol. **39:**519–529.
16. **Fukuchi, K., M. Sudo, Y.-S. Lee, A. Tanaka, and M. Nonoyama.** 1984. Structure of Marek's disease virus DNA: detailed restriction enzyme map. J. Virol. **51:**102–109.
17. **Georgopoulou, U., A. Michaelidou, B. Roizman, and P. Mavromara-Nazos.** 1993. Identification of a new transcription unit that yields a gene product within the unique sequences of the short component of the herpes simplex virus 1 genome. J. Virol. **67:** 3961–3968.
18. **Holden, V. R., R. R. Yalamanchili, R. N. Harty, and D. J. O'Callaghan.** 1992. ICP22 homolog of equine herpesvirus 1: expression from early and late promoters. J. Virol. **66:**664–673.
19. **Holden, V. R., R. R. Yalamanchili, R. N. Harty, and D. J. O'Callaghan.** 1992. Identification and characterization of an equine herpesvirus 1 late gene encoding a potential zinc finger. Virology **188:**704–713.
20. **Jackers, P., P. Defechereux, L. Baudoux, C. Lambert, M. Massaer, M.-P. Merville-Louis, B. Rentier, and J. Piette.** 1992. Characterization of regulatory functions of the varicella-zoster virus gene 63-encoded protein. J. Virol. **66:**3899–3903.
21. **Longnecker, R., and B. Roizman.** 1986. Generation of an inverting herpes simplex virus 1 mutant lacking the L-S junction *a* sequences, an origin of DNA synthesis, and several genes including those specifying glycoprotein E and the α47 gene. J. Virol. **58:** 583–591.
22. **Longnecker, R., and B. Roizman.** 1987. Clustering of genes dispensable for growth in culture in the S component of the HSV-1 genome. Science **236:**573–576.
23. **McGeoch, D. J.** 1989. The genomes of the human herpesviruses: contents, relationships and evolution. Annu. Rev. Microbiol. **43:** 235–265.
24. **McGeoch, D. J., A. Dolan, S. Donald, and F. J. Rixon.** 1985. Sequence determination and genetic content of the short unique region of the genome of herpes simplex type 1. J. Mol. Biol. **181:** 1–13.
25. **McGeoch, D. J., H. W. M. Moss, D. McNab, and M. C. Frame.** 1987. DNA sequence and genetic content of the *Hin*dIII L region in the short unique component of the herpes simplex virus type 2 genome: identification of the gene encoding glycoprotein G, and evolutionary comparisons. J. Gen. Virol. **68:**19–38.
26. **Mettenleiter, T. C., C. Schreurs, F. Zuckermann, T. Ben-Porat, and A. S. Kaplan.** 1988. Role of glycoprotein gIII of pseudorabies virus in virulence. J. Virol. **62:**2712–2717.
27. **Morgan, R. W., J. L. Cantello, and C. H. McDermott.** 1990. Transfection of chicken embryo fibroblasts with Marek's disease virus DNA. Avian Dis. **34:**345–351.
28. **Parcells, M. S., A. S. Anderson, and R. W. Morgan.** Characterization of a Marek's disease virus mutant containing a *lacZ* insertion in the US6 (gD) homologue gene. Virus Genes, in press.
29. **Parcells, M. S., and R. W. Morgan.** Unpublished data.
30. **Poffenberger, K. L., P. E. Raichlen, and R. C. Herman.** 1993. In vitro characterization of a herpes simplex virus type 1 ICP22 deletion mutant. Virus Genes **7:**171–186.
31. **Post, L. E., and B. Roizman.** 1981. A generalized technique for deletion of specific genes in large genomes: α gene 22 of herpes simplex virus is not essential for growth. Cell **25:**227–232.
32. **Purves, F. C., and B. Roizman.** 1992. The herpes simplex virus 1 U_L13 gene encodes the functions for post-translational processing associated with phosphorylation of the regulatory protein α 22. Proc. Natl. Acad. Sci. USA **89:**7310–7314.
33. **Ross, L. J. N., M. M. Binns, and J. Pastorek.** 1991. DNA sequence and organization of genes in a 5.5 kbp EcoRI fragment mapping in the short unique segment of Marek's disease (strain RB1B). J. Gen. Virol. **72:**949–954.
34. **Sakaguchi, M., T. Urakawa, Y. Hirayama, N. Miki, M. Yamamoto, G.-S. Zhu, and K. Hirai.** 1993. Marek's disease virus protein kinase gene identified within the short unique region of the viral genome is not essential for viral replication in cell culture and vaccine-induced immunity in chickens. Virology **195:**140–148.
35. **Sakaguchi, M., T. Urakawa, Y. Hirayama, N. Miki, M. Yamamoto, and K. Hirai.** 1992. Sequence determination and genetic content of an 8.9-kb restriction fragment in the short unique region and the internal inverted repeat of Marek's disease virus type I DNA. Virus Genes **6:**365–378.
36. **Sambrook, J., E. F. Fritsch, and T. Maniatis.** 1989. Molecular cloning: a laboratory manual, 2nd ed. Cold Spring Harbor Laboratory, Cold Spring Harbor, N.Y.
37. **Schat, K. A., A. Buckmaster, and L. J. N. Ross.** 1989. Partial transcription map of Marek's disease herpesvirus in lytically infected and lymphoblastoid cells. Int. J. Cancer **44:**101–109.
38. **Schwyzer, M., C. Vlcek, O. Menekse, C. Fraefel, and V. Paces.** 1993. Promoter, spliced leader, and coding sequence for BICP4, the largest of the immediate-early proteins of bovine herpesvirus 1. Virology **197:**349–357.
39. **Sears, A. E., I. W. Halliburton, B. Meignier, S. Silver, and B. Roizman.** 1985. Herpes simplex virus 1 mutant deleted in the α22 gene: growth and gene expression in permissive and restrictive cells and establishment of latency in mice. J. Virol. **55:**338–346.
40. **Sondermeijer, P. J. A., J. A. J. Claessens, P. E. Jenniskens, A. P. A.**

Mockett, R. A. J. Thijssen, M. J. Willemse, and R. W. Morgan. 1993. Avian herpesvirus as a live viral vector for the expression of heterologous antigens. Vaccine **11**:349–358.

41. **Telford, E. A. R., M. S. Watson, K. McBride, and A. J. Davison.** 1992. The DNA sequence of equine herpesvirus-1. Virology **189**: 304–316.
42. **Umene, K.** 1986. Conversion of a fraction of the unique sequence to part of the inverted repeats in the S component of the herpes simplex virus type 1 genome. J. Gen. Virol. **67**:1035–1048.
43. **van Zijl, M., H. van der Gulden, N. de Wind, A. Gielkens, and A. Berns.** 1990. Identification of two genes in the unique short region of pseudorabies virus; comparison with herpes simplex virus and varicella-zoster virus. J. Gen. Virol. **71**:1747–1755.
44. **Weber, P. C., M. Levine, and J. C. Glorioso.** 1987. Rapid identification of nonessential genes of herpes simplex virus type 1 by Tn5 mutagenesis. Science **236**:576–579.
45. **Whitton, J. L., and J. B. Clements.** 1984. The junctions between the repetitive and the short unique sequences of the herpes simplex virus genomes are determined by the polypeptide-coding regions of two spliced immediate-early mRNAs. J. Gen. Virol. **65**: 451–466.
46. **Zelnik, V., R. Darteil, J. C. Audonnet, G. D. Smith, M. Riviere, J. Pastorek, and L. J. N. Ross.** 1993. The complete sequence and gene organization of the short unique region of herpesvirus of turkeys. J. Gen. Virol. **74**:2151–2162.
47. **Zhang, G., and D. P. Laeder.** 1990. The structure of the pseudorabies virus genome at the end of the inverted repeat sequences proximal to the junction with the short unique region. J. Gen. Virol. **71**:2433–2441.